Oppositely rotating eigenmodes of spin-polarized current-driven vortex gyrotropic motions in elliptical nanodots

Ki-Suk Lee, Young-Sang Yu, Youn-Seok Choi, Dae-Eun Jeong, and Sang-Koog Kim

---

Articles you may be interested in

Understanding eigenfrequency shifts observed in vortex gyrotropic motions in a magnetic nanodot driven by spin-polarized out-of-plane dc current
Appl. Phys. Lett. **93**, 182508 (2008); 10.1063/1.3012380

Reliable low-power control of ultrafast vortex-core switching with the selectivity in an array of vortex states by in-plane circular-rotational magnetic fields and spin-polarized currents
Appl. Phys. Lett. **92**, 022509 (2008); 10.1063/1.2807274

Gyrotropic linear and nonlinear motions of a magnetic vortex in soft magnetic nanodots
Appl. Phys. Lett. **91**, 132511 (2007); 10.1063/1.2783272

Spin-polarized current-driven switching in permalloy nanostructures
J. Appl. Phys. **97**, 10E302 (2005); 10.1063/1.1847292

Circular domain wall motion driven by spin-polarized currents in confined square nanomagnets
J. Appl. Phys. **97**, 044306 (2005); 10.1063/1.1847725

Oppositely rotating eigenmodes of spin-polarized current-driven vortex gyrotropic motions in elliptical nanodots

Ki-Suk Lee, Young-Sang Yu, Youn-Seok Choi, Dae-Eun Jeong, and Sang-Koog Kim[a)]

Research Center for Spin Dynamics and Spin-Wave Devices and Nanospinics Laboratory,
Department of Materials Science and Engineering, College of Engineering, Seoul National University,
Seoul 151-744, Republic of Korea

The authors found that there exist two different rotational eigenmodes of oppositely rotating sense in spin-polarized current-driven vortex gyrotropic motions in soft magnetic elliptical nanodots. Simple mathematical expressions were analytically calculated by adopting vortex-core (VC)-rotation-sense-dependent dynamic susceptibility tensors based on the linearized Thiele equation [Phys. Rev. Lett. **30**, 230 (1973)]. The numerical calculations of those analytical expressions were confirmed by micromagnetic simulations, revealing that linear-regime steady-state VC motions driven by any polarized oscillating currents can be interpreted simply by the superposition of the clockwise and counterclockwise rotational eigenmodes. The shape of the orbital trajectories of the two eigenmodes is determined only by the lateral dimension of elliptical dots. Additionally, the orbital radii and phases of the two eigenmodes' VC motions were found to markedly vary with the frequency of applied currents, particularly across the vortex eigenfrequency and according to the vortex polarization, which results in overall VC motions driven by any polarized oscillating currents. © 2008 American Institute of Physics. [DOI: 10.1063/1.2926666]

In micron-size (or smaller) magnetic elements such as circular, square, or rectangular nanodots, the in-plane curling magnetization ($\mathbf{M}$) configuration (concentric circle) along with the out-of-plane $\mathbf{M}$ orientation at the center region are found to be in a ground state, the so-called magnetic vortex (MV). Following upon the initial experimental observations of this peculiar static structure in such restricted geometry[1] or continuous thin films,[2] various nontrivial dynamic modes of vortex excitations have been found both theoretically[3,4] and experimentally.[5] One of the excited modes with a vortex state is the translation motion of a vortex core (VC) in the dot plane, the so-called gyrotropic motion.[3] This responsible motion is due to the gyroforce being in balance with the restoring force caused by dipole-dipole interaction in confined nanoelements. When the frequency of an oscillating magnetic field or current reaches the characteristic eigenfrequency of a vortex, typically several hundred megahertz,[3–7] the VC is resonantly excited and reaches a steady-state rotational motion.[7–12] More recently, in our previous studies, we have shown, by micromagnetic numerical calculations, that there exist counterclockwise (CCW) and clockwise (CW) circular rotational VC motions driven by the corresponding CCW and CW rotational fields or currents and that their rotational motions' orbital radius amplitudes are remarkably contrasting in magnitude and are reversed by changing the VC $\mathbf{M}$ orientation (polarization).[11] Only one of these oppositely rotational motions, depending on the vortex polarization, attains VC switching. This selective core switching by means of one or the other circularly polarized acs (or fields) thus becomes an emerging core technology, promisingly applicable to vortex random access memory or sensor devices.[12] Therefore, it is necessary to clearly understand the underlying physics of the rotational gyrotropic vortex motions observed in previous micromagnetic numerical simulations. In this letter, we report on theoretically derived simple mathematical expressions of the two opposite rotational VC motions and their asymmetric resonance, in order to gain insight into their physical properties. Those mathematical expressions provide information on how linear-regime steady-state vortex motions vary with the polarization of a given vortex state as well as the driving force frequency, and thereby point to the practical implementations of vortex-based information storage and sensor devices.

Based on the linearized Thiele equation,[13] we analytically calculated the linear-regime VC motions,[14] each driven by either the CCW or CW elliptically or circularly polarized oscillating currents, $\mathbf{j}_{\mathrm{CCW,CW}} = j_0[\pm\cos(\omega_\mathbf{I}t)\hat{\mathbf{x}} + \eta\sin(\omega_\mathbf{I}t)\hat{\mathbf{y}}]$, where ω_I is the angular frequency, j_0 is the amplitude of the oscillating current density, and $\eta = r_y/r_x$ is the ratio of the lengths of two semi-axes of a given elliptical dot, as defined in Fig. 1(a), where $\eta = 1$ indicates the circular dot geometry. Additionally, to confirm the analytical derivation, micromagnetic simulations were carried out by using the LLG code.[15]
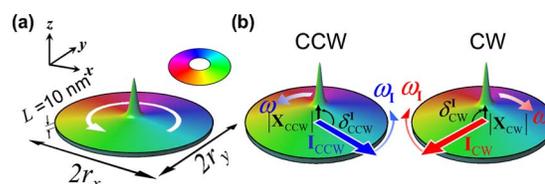

FIG. 1. (Color online) (a) Elliptical dot geometry along with the ground state $\mathbf{M}$ distribution, for example, of the upward-core $\mathbf{M}$ orientation and CCW in-plane $\mathbf{M}$ rotation around its VC under no driving force. The color and height display the local in-plane $\mathbf{M}$ orientation, as indicated by the color wheel, as well as the out-of-plane $\mathbf{M}$ components, respectively. (b) Graphical illustrations of the CCW and CW rotational eigenmodes and the corresponding elliptically rotating currents, $\mathbf{I}_{\mathrm{CCW}}$ and $\mathbf{I}_{\mathrm{CW}}$, in an elliptical dot. The radius amplitude $|\mathbf{X}_{\mathrm{CCW,CW}}|$ and phase $\delta^{\mathbf{I}}_{\mathrm{CCW,CW}}$ of the steady-state VC motions' orbits for the CCW and CW rotational eigenmodes are defined as described in the text.

a)Author to whom correspondence should be addressed. Electronic mail: sangkoog@snu.ac.kr.

As seen in Fig. 1(a), the model systems used here are circular and elliptical dots made of Permalloy (Py), with lateral dimensions $2r_x \times 2r_y = 300 \times 300$, 300×150, and 450×150 nm^2 and of the same thickness $L = 10$ nm. For the given restricted Py dots, the spatial **M** configurations are illustrated, for example, as a single MV with the up-core orientation represented by the polarization $p = 1$ and with the chirality $C = 1$ represented by the CCW in-plane **M** rotation. The characteristic eigenfrequency[3] of a vortex state in each geometry is determined to be $\nu_D = \omega_D / 2\pi = 330$, 380, and 250 MHz for $2r_x \times 2r_y = 300 \times 300$, 300×150, and 450×150 nm^2, respectively. Details of the material parameters for the analytical calculations and simulations were given in our previous studies.[8,12]

For a VC motion from its initial position $\mathbf{X} = (X, Y) = 0$, a linearized Thiele equation, including a driving force by spin-polarized currents,[16] is written as $\mathbf{G} \times \dot{\mathbf{X}} - \mathbf{G} \times \mathbf{v}_S + \hat{D}\dot{\mathbf{X}} - \partial W(\mathbf{X}, t)/\partial \mathbf{X} = 0$, where $\mathbf{G} = -G\hat{\mathbf{z}}$ is the gyrovector with the gyrovector constant G (Ref. 3), and $\hat{D} = D\hat{I}$ is the damping tensor with the identity matrix $\hat{I}$ and the damping constant D (Ref. 10). $\mathbf{v}_S$ is the drift velocity of electron spins and is given as $\mathbf{v}_S = -Pa^3\mathbf{j}/(2eS)$,[17] where P is the spin polarization, a is the lattice constant, e is the absolute value of electronic charge, and S is the magnitude of spin. For a general elliptical geometry, the potential energy is given as $W(\mathbf{X}, t) = W(0) + \kappa_x X^2/2 + \kappa_y Y^2/2$,[18] where $W(0)$ is the potential energy corresponding to $\mathbf{X} = 0$, and the second and third terms are dominated by the exchange—magnetostatic energies for the VC shift from $\mathbf{X} = 0$ to the x- and y-directions, respectively, with the corresponding stiffness coefficients κ_x and κ_y. Then, the linearized Thiele equation for the spin-polarized current-driven vortex motion is rewritten as $\mathbf{G} \times \dot{\mathbf{X}} + \hat{D}\dot{\mathbf{X}} - \kappa_x X\hat{\mathbf{x}} - \kappa_y Y\hat{\mathbf{y}} + \mu_{\mathbf{I}}(\hat{\mathbf{z}} \times \mathbf{j}) = 0$, with $\mu_{\mathbf{I}} = -p|G|Pa^3/(2eS)$.

For arbitrary polarized oscillating currents $\mathbf{j} = \mathbf{j}_0 \exp(-i\omega_{\mathbf{I}} t)$, the solution of the linearized Thiele equation is given by $\mathbf{X} \simeq \mathbf{X}_0 \exp(-i\omega_{\mathbf{I}} t)$ for the case of a linear-regime steady-state motion,[9] where $\mathbf{X}_0$ can be obtained from the dynamic susceptibility tensor $\hat{\chi}_{\mathbf{X}}(\omega_{\mathbf{I}})$ (Ref. 11) through the relation $\mathbf{X}_0 = \hat{\chi}_{\mathbf{X}}(\omega_{\mathbf{I}})\mathbf{j}_0$. In the $(x$-$y)$ dot plane, a 2×2 matrix dynamic susceptibility tensor is given as

$$\hat{\chi}_{\mathbf{X},L}(\omega_{\mathbf{I}}) = \frac{\mu_{\mathbf{I}}}{(i\omega_{\mathbf{I}}D + \kappa_x)(i\omega_{\mathbf{I}}D + \kappa_y) - (\omega_{\mathbf{I}}G)^2}$$
$$\times \begin{bmatrix} -i\omega_{\mathbf{I}}G & -(i\omega_{\mathbf{I}}D + \kappa_y) \\ (i\omega_{\mathbf{I}}D + \kappa_x) & -i\omega_{\mathbf{I}}G \end{bmatrix}. \quad (1)$$

The diagonalization of $\hat{\chi}_{\mathbf{X},L}$ with respect to the elliptical basis of $\hat{\mathbf{e}}_{\text{CCW,CW}} = (\beta_y\hat{\mathbf{x}} \pm i\beta_x\hat{\mathbf{y}})/\sqrt{\beta_x^2 + \beta_y^2}$, with $\beta_{x,y} = \sqrt{i\omega_{\mathbf{I}}D + \kappa_{x,y}}$, allows us to obtain the diagonal susceptibility tensor $\hat{\chi}_{\mathbf{X},E} = \begin{pmatrix} \chi_{\text{CCW}} & 0 \\ 0 & \chi_{\text{CW}} \end{pmatrix}$ with respect to an elliptical eigenbasis. For an elliptical geometry with submicron lateral dimensions and of a few tens of nanometer thickness, we can assume that $\kappa_y b^2 = a^2\kappa_x$ and $\omega D \ll \kappa_{x,y}$.[18] Thus, the elliptical eigenvectors are given by $\hat{\mathbf{e}}_{\text{CCW,CW}} = (r_x\hat{\mathbf{x}} \pm ir_y\hat{\mathbf{y}})/\sqrt{r_x^2 + r_y^2}$, being equal to the same aspect ratio as that of the given elliptical geometry. Consequently, the mathematical expressions of the two rotational eigenmodes are as follows:

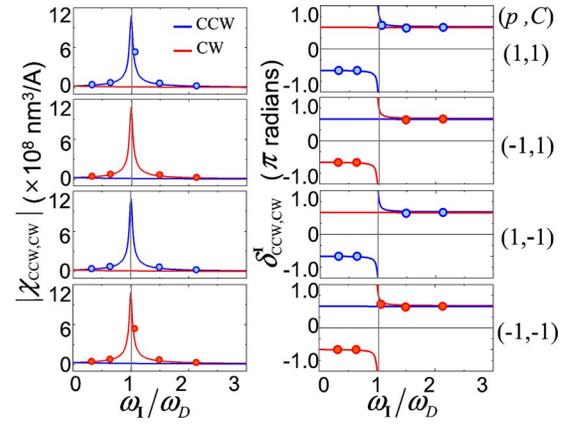$$\mathbf{X}_{\text{CCW}}(t) = X_{0,\text{CCW}}\hat{\mathbf{e}}_{\text{CCW}} \exp(-i\omega_{\mathbf{I}} t)$$

and

FIG. 2. (Color online) Numerical calculations of the analytical equations (solid lines) of $|\chi_{\text{CCW,CW}}|$ and $\delta_{\text{CCW,CW}}^{\mathbf{I}}$ vs $\omega_{\mathbf{I}}/\omega_D$ for a given polarization and chirality (p, C), as noted, in a circular dot of $2r_x \times 2r_y = 300 \times 300$ nm^2. The analytical results are compared to the micromagnetic simulations (circle symbols) for the CCW (blue) and CW (red) eigenmodes in response to the pure circular currents, $\mathbf{j}_{\text{CCW}}$ and $\mathbf{j}_{\text{CW}}$, respectively. In the simulations, $|\chi_{\text{CCW,CW}}|$ was estimated from $|\mathbf{X}_{\text{CCW,CW}}|/|\mathbf{j}_{\text{CCW,CW}}|$.

$$\mathbf{X}_{\text{CW}}(t) = X_{0,\text{CW}}\hat{\mathbf{e}}_{\text{CW}} \exp(-i\omega_{\mathbf{I}} t),$$

where

$$\mathbf{X}_{0,E} = X_{0,\text{CCW}}\hat{\mathbf{e}}_{\text{CCW}} + X_{0,\text{CW}}\hat{\mathbf{e}}_{\text{CW}} = \begin{pmatrix} \chi_{\text{CCW}} & 0 \\ 0 & \chi_{\text{CW}} \end{pmatrix}\mathbf{j}_{0,E},$$

with

$$\mathbf{j}_{0,E} = j_{0,\text{CCW}}\hat{\mathbf{e}}_{\text{CCW}} + j_{0,\text{CW}}\hat{\mathbf{e}}_{\text{CW}}$$

and

$$\chi_{\text{CCW,CW}} = i\mu_{\mathbf{I}}/[\omega_{\mathbf{I}}G \mp \sqrt{(i\omega D + \kappa_x)(i\omega D + \kappa_y)}].$$

For the simplest (most convenient) circular dot geometry case, assuming $r_x = r_y$ and $\kappa_x = \kappa_y = \kappa$, the circular eigenbasis and corresponding dynamic susceptibility tensor are given by $\hat{\mathbf{e}}_{\text{CCW,CW}} = \frac{1}{\sqrt{2}}(\hat{\mathbf{x}} \pm i\hat{\mathbf{y}})$ and $\chi_{\text{CCW,CW}} = i\mu_{\mathbf{I}}/[\omega_{\mathbf{I}}G \mp (i\omega_{\mathbf{I}}D + \kappa)]$, respectively. In this case, the measurable useful quantities of the magnitude and phase of $\chi_{\text{CCW,CW}}$ can be rewritten as

$$|\chi_{\text{CCW,CW}}| = |\mu_{\mathbf{I}}|/\sqrt{(G^2 + D^2)(\omega_{\mathbf{I}} \mp p\omega_D)^2 + \kappa^2D^2/(G^2 + D^2)}, \quad (2a)$$

$$\delta_{\text{CCW,CW}}^{\mathbf{I}} = -\tan^{-1}[(\kappa \mp p\omega_{\mathbf{I}}|G|)/(\omega_{\mathbf{I}}D)] + \frac{\pi}{2}(1 \pm p), \quad (2b)$$

where $\omega_D = \kappa|G|/(G^2 + D^2)$. Both $|\chi_{\text{CCW,CW}}|$ and $\delta_{\text{CCW,CW}}^{\mathbf{I}}$ depend only on p, independent of C.[19] The numerical calculations of Eqs. (2a) and (2b) are plotted versus $\omega_{\mathbf{I}}/\omega_D$ for each of the two opposite eigenmodes, according to the four different cases of (p, C), as seen in Fig. 2. The analytical results are in excellent agreement with the corresponding micromagnetic simulations (circle symbols).

From the results shown in Fig. 2, we derive the following conclusions. (1) There are two rotational eigenmodes in restricted-geometry vortex gyrotropic motions; (2) both $|\chi_{\text{CCW,CW}}|$ and $\delta_{\text{CCW,CW}}^{\mathbf{I}}$ vary with $\omega_{\mathbf{I}}/\omega_D$, showing strong resonance effects at $\omega_{\mathbf{I}}/\omega_D = 1$ for one of the two opposite rotational eigenmodes; (3) the two eigenmodes' resonances are asymmetric, that is, only one, either the CCW or the CW motion, shows a resonance behavior, the other showing non-
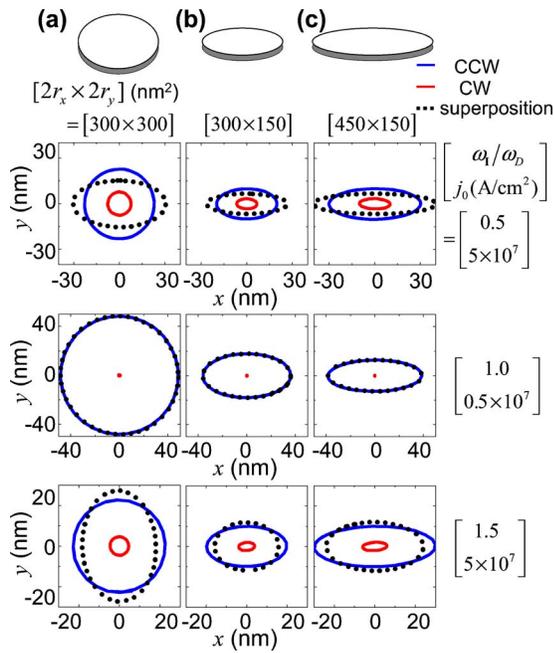
FIG. 3. (Color online) Calculations of the orbital trajectories of the CCW and CW eigenmodes' VC motions in the indicated dot geometries, driven by the corresponding eigenbasis currents, $\mathbf{j}_{CCW}$ (blue solid line) and $\mathbf{j}_{CW}$ (red solid line), as well as their superposition results (black dotted line), with $j_0 = 5 \times 10^7 \, A/cm^2$ for $\omega_I/\omega_D = 0.5$ and 1.5, and $j_0 = 0.5 \times 10^7 \, A/cm^2$ for $\omega_I/\omega_D = 1$, for a specific case of $(p, C) = (+1, +1)$.

resonance; (4) the mode showing the resonance effect switches according to the vortex polarization; and (5) the variation of $\delta^{\mathbf{I}}$ with ω_I/ω_D switches between the CCW and CW eigenmodes according to the vortex polarization, because the exertion of a current-driven force on the vortex depends on p, but not on C.

　　To reproduce the observed vortex gyrotropic motions, we plotted the orbital trajectories of the CCW and CW eigenmodes with respect to the elliptical- and circular-rotational currents, $\mathbf{j}_{CCW}$ and $\mathbf{j}_{CW}$, as well as their superposition corresponding to the responses to linearly oscillating currents, in this case, $\mathbf{j}_{lin}$ along the y-axis. In the calculations, we used the case of $(p, C) = (+1, +1)$ for different values, $\omega_I/\omega_D = 0.5$, 1.0, and 1.5. To avoid nonlinear vortex excitations,[14,20] we used a relatively low-current-density amplitude. The shapes of the orbital trajectories of the individual CCW and CW rotational motions were the same as that of the lateral dimensions of the given elliptical dot and were not changed, but the magnitudes were changed with ω_I/ω_D. However, the orbital shapes of the superposition of the oppositely rotating eigenmotions, corresponding to the motion in response to $\mathbf{j}_{lin}$, were changed with ω_I/ω_D owing to both the $|\chi_{CCW,CW}|$ and the $\delta^{\mathbf{I}}_{CCW,CW}$ dependences on ω_I/ω_D, as shown in Fig. 2. For example, for $\omega_I < \omega_D$, the phases of the opposite eigenmodes were given as $\delta^{\mathbf{I}}_{CCW} = -\pi/2$ and $\delta^{\mathbf{I}}_{CW} = \pi/2$, i.e., out of phase, while in the case of $\omega_I > \omega_D$, they were the same, such that $\delta^{\mathbf{I}}_{CCW} = \delta^{\mathbf{I}}_{CW} = \pi/2$, i.e., in phase. The phase difference between the CCW and CW rotational eigenmodes makes the shape of the orbital trajectory of their superposition different

from that of the individual eigenmodes, as shown in Fig. 3.

　　In summary, we analytically solved the CCW and CW rotational eigenmodes of vortex gyrotropic motions driven by spin-polarized currents. Between the two opposite eigenmodes, there exists an asymmetric resonance effect, that is, strong resonance for only the CCW rotational eigenmode at $\omega_I = \omega_D$ and nonresonance for the other CW eigenmode, for the up-core orientation, but vice versa for the down-core orientation. These mathematical expressions inform us how spin-polarized current-driven linear-regime steady-state vortex motions vary with the polarization of a given vortex state as well as the frequency of applied currents.

[1] T. Shinjo, T. Okuno, R. Hassdorf, K. Shigeto, and T. Ono, Science **289**, 930 (2000); A. Wachowiak, J. Wiebe, M. Bode, O. Pietzsch, M. Morgenstern, and R. Wiesendanger, *ibid.* **298**, 577 (2002).

[2] S.-K. Kim, J. B. Kortright, and S.-C. Shin, Appl. Phys. Lett. **78**, 2742 (2001); S.-K. Kim, K.-S. Lee, B.-W. Kang, K.-J. Lee, and J. B. Kortright, *ibid.* **86**, 052504 (2005).

[3] K. Y. Guslienko, B. A. Ivanov, V. Novosad, Y. Otani, H. Shima, and K. Fukamichi, J. Appl. Phys. **91**, 8037 (2002).

[4] Y. B. Gaididei, V. P. Kravchuk, F. G. Mertens, and D. D. Sheka, arXiv:cond-mat/0801.4045v2.

[5] J. P. Park, P. Eames, D. M. Engebretson, J. Berezovsky, and P. A. Crowell, Phys. Rev. B **67**, 020403(R) (2003); S. B. Choe, Y. Acremann, A. Scholl, A. Bauer, A. Doran, J. Stohr, and H. A. Padmore, Science **304**, 420 (2004); R. Antos, Y. Otani, and J. Shibata, J. Phys. Soc. Jpn. **77**, 031004 (2008).

[6] K. Y. Guslienko, X. F. Han, D. J. Keavney, R. Divan, and S. D. Bader, Phys. Rev. Lett. **96**, 067205 (2006).

[7] S. Kasai, Y. Nakatani, K. Kobayshi, H. Kohno, and T. Ono, Phys. Rev. Lett. **97**, 107204 (2006).

[8] S.-K. Kim, Y.-S. Choi, K.-S. Lee, K. Y. Guslienko, and D.-E. Jeong, Appl. Phys. Lett. **91**, 082506 (2007).

[9] B. Kruger, A. Drews, M. Bolte, U. Merkt, D. Pfannkuche, and G. Meier, Phys. Rev. B **76**, 224426 (2007).

[10] K. Y. Guslienko, Appl. Phys. Lett. **89**, 022510 (2006).

[11] K.-S. Lee and S.-K. Kim, "Two circular-rotational eigenmodes and their giant resonance asymmetry in vortex gyrotropic motions in soft magnetic circular nanodots," Phys. Rev. B (in press); K.-S. Lee, D.-E. Jeong, Y.-S. Choi, Y.-S. Yu, K. Y. Guslienko, and S.-K. Kim, The 52nd MMM Conference, Tampa, 2007 (unpublished), p. HC-13.

[12] S.-K. Kim, K.-S. Lee, Y.-S. Yu, and Y.-S. Choi, Appl. Phys. Lett. **92**, 022509 (2008).

[13] A. A. Thiele, Phys. Rev. Lett. **30**, 230 (1973); D. L. Huber, Phys. Rev. B **26**, 3758 (1982).

[14] K.-S. Lee and S.-K. Kim, Appl. Phys. Lett. **91**, 132511 (2007).

[15] See http://llgmicro.home.mindspring.com/

[16] L. Berger, Phys. Rev. B **54**, 9353 (1996); J. C. Slonczewski, J. Magn. Magn. Mater. **159**, L1 (1996).

[17] S. Zhang and Z. Li, Phys. Rev. Lett. **93**, 127204 (2004); A. Thiaville, Y. Nakatani, J. Miltat, and Y. Suzuki, Europhys. Lett. **69**, 990 (2005); J. Shibata, Y. Nakatani, G. Tatara, H. Kohno, and Y. Otani, Phys. Rev. B **73**, 020403 (2006).

[18] K. S. Buchanan, P. E. Roy, M. Grimsditch, F. Y. Fradin, K. Y. Guslienko, S. D. Bader, and V. Novosad, Phys. Rev. B **74**, 064404 (2006); K. S. Buchanan, P. E. Roy, F. Y. Fradin, K. Y. Guslienko, M. Grimsditch, S. D. Bader, and V. Novosad, J. Appl. Phys. **99**, 08C707 (2006).

[19] For the case of oscillating fields, $|\chi_{CCW,CW}|$ depends only on p, but $\delta_{CCW,CW}$ depends on both p and C. For details, see Ref. 11.

[20] K. S. Buchanan, M. Grimsditch, F. Y. Fradin, S. D. Bader, and V. Novosad, Phys. Rev. Lett. **99**, 267201 (2007).